




Plasma complement C7 as a target in non-small cell lung cancer patients to implement 3P medicine strategies

Jae Gwang Park^{1,2} · Beom Kyu Choi³ · Youngjoo Lee⁴ · Eun Jung Jang^{1,5} · Sang Myung Woo^{3,5,6} · Jun Hwa Lee¹ · Kyung-Hee Kim^{5,7} · Heeyoun Hwang⁸ · Wonyoung Choi⁹ · Se-Hoon Lee¹⁰ · Byong Chul Yoo^{1,5} 

Received: 14 October 2021 / Accepted: 4 November 2021 / Published online: 25 November 2021

© The Author(s), under exclusive licence to European Association for Predictive, Preventive and Personalised Medicine (EPMA) 2021

Abstract

Background Programmed cell death-1 (PD-1)/programmed cell death ligand-1 (PD-L1) immune checkpoint inhibitors (ICIs) significantly affect outcomes in non-small cell lung cancer (NSCLC) patients. However, differences in reactions toward PD-1/PD-L1 ICI among patients impose inefficient treatment. Therefore, developing a reliable biomarker to predict PD-1/PD-L1 ICI reaction is highly necessary for predictive, preventive, and personalized (3P) medicine.

Materials and methods We recruited 63 patients from the National Cancer Center (NCC) and classified them into the training and validation sets. Next, 99 patients were recruited for inclusion into the external validation set at the Samsung Medical Center (SMC). Proteomic analysis enabled us to identify plasma C7 levels, which were significantly different among groups classified by their overall response to the RECIST V 1.1–based assessment. Analytical performance was evaluated to predict the PD-1/PD-L1 ICI response for each type of immunotherapy, and NSCLC histology was evaluated by determining the C7 levels via ELISA.

Results Plasma C7 levels were significantly different between patients with and without clinical benefits (PFS \geq 6 months). Among the groups sorted by histology and PD-1/PD-L1 immunotherapy type, only the predicted accuracy for pembrolizumab-treated patients from both NCC and SMC was greater than 73%. In patients treated with pembrolizumab, C7 levels were superior to those of the companion diagnostics 22C3 (70.3%) and SP263 (62.1%). Moreover, for pembrolizumab-treated patients for whom the PD-L1 tumor proportion score (TPS) was $<$ 50%, the predictive accuracy of C7 was nearly 20% higher than that of 22C3 and SP263.

Conclusion Evaluation of plasma C7 levels shows an accurate prediction of NSCLC patient reactions on pembrolizumab. It demonstrates plasma C7 is an alternative and supportive biomarker to overcome the predictive limitation of previous 22C3 and SP263. Thus, it is clear that clinical use of plasma C7 allows predictive diagnosis on lung cancer patients who have not been successfully treated with current CDx and targeted prevention on metastatic diseases in secondary care caused by a misdiagnosis of current CDx. Reduction of patients' financial burden and increased efficacy of cancer treatment would also enable prediction, prevention, and personalization of medical service on NSCLC patients. In other words, plasma C7 provides efficient medical service and an optimized medical economy followed which finally promotes the prosperity of 3P medicine.

Keywords Non-small cell lung cancer · Biomarkers · Complement component 7 · Pembrolizumab · Predictive preventive personalized medicine (3P medicine/3PM/PPPM) · Patient stratification · Targeted treatment · Improved individual outcomes

Jae Gwang Park, Beom Kyu Choi and Youngjoo Lee are co-first authors.

✉ Se-Hoon Lee
shlee119@skku.edu

✉ Byong Chul Yoo
yoo_akh@ncc.re.kr

Extended author information available on the last page of the article

Introduction

The advent of immunotherapy for the treatment of non-small cell lung cancer (NSCLC) patients by using immune checkpoint inhibitors (ICIs) of programmed cell death protein-1 (PD-1)/programmed cell death ligand-1 (PD-L1) has significantly ameliorated the burden of disease for NSCLC patients [1, 2]. PD-1/PD-L1 immune checkpoint inhibitors such as

nivolumab, pembrolizumab, atezolizumab, and durvalumab have been approved by the US FDA for the treatment of advanced NSCLC patients after first-line therapy. Each of these four agents reportedly increased the progression-free survival (PFS) and overall survival (OS) of NSCLC patients, compared to chemotherapy [3, 4]. Recently, the US FDA approved the use of pembrolizumab and atezolizumab for the first-line treatment of patients with stage III NSCLC, for whom it was not feasible to perform surgery or chemoradiation [5, 6]. Clinical trials (CheckMate 057, CheckMate 017, KEYNOTE-010, POPLAR, and OAK) for each of these agents were closely associated with the degree of clinical efficacy and tumoral PD-1/PD-L1 expression levels, assessed by PD-1/PD-L1 immunohistochemistry [7–10].

Companion diagnostics (CDx) to predict PD-1/PD-L1 ICI response in NSCLC

The results of these clinical trials suggested that the ability to predict the response of a patient to a particular drug can avert treatment failure resulting from the administration of a physically or financially ineffective treatment. Hence, the application of companion diagnostics (CDx) has been approved in the USA, Europe, and other countries. Clone 22C3 has been approved by the US FDA as a CDx for assessing whether advanced NSCLC patients should be treated with pembrolizumab, while clone 28–8 has been recommended as a CDx for assessing whether patients should be treated with nivolumab after chemotherapy [11]. In Europe, the clone 22C3 assay was designated as a CE-IVD and CDx for treatment with durvalumab, pembrolizumab, and nivolumab. In addition, clone SP263, designated as a CE-IVD, is a CDx for pembrolizumab monotherapy [12].

Limitations of current CDx for PD-1/PD-L1 ICI

Although the use of the PD-1/PD-L1 expression level as a CDx tool has been approved in various countries, CDx have certain drawbacks. CDx relying on PD-1/PD-L1 expression sometimes showed low levels of efficacy, in comparison to that of well-known diagnostics, because the expression of PD-1/PD-L1 differed with the cancer type [13, 14].

In general, CDx involve the staining of tissues obtained through endoscopic bronchial and transthoracic needle biopsy, via a current method. Since a biopsy can be used to extract only a limited amount of tissue, it is difficult to obtain tissues in which the biomarker is uniformly distributed. The amount of PD-1/PD-L1-stained tumor cells was not similar even among tissues excised from the same lung cancer patient [15]. Moreover, invasive tissue biopsy further entails various complications such as bleeding or pain which aggravate risks on patients and medical representatives.

Second, mutations within tumors, chronological changes, and microenvironment-related differences often impair the functioning of various biomarkers. Although the tumor mutation burden (TMB) is widely correlated with the patient survival and ICI treatment response, an abundant TMB affects the accuracy of PD-1/PD-L1-mediated companion diagnosis in NSCLC patients [16].

Lastly, the currently used process of companion diagnosis is commercialized and requires expensive equipment, such as an automatic staining device. Hence, several laboratories have performed studies to devise methods that do not involve the use of expensive equipment [17, 18].

Needs to develop a new alternative biomarker for implementing predictive, preventive, and personalized (3P) medicine of NSCLC patients treated by PD-1/PD-L1 ICI

PD-1/PD-L1 ICI causes the extinction of tumor cells by helping its immunogenicity at a high level and inducing activation of immune cells around [19, 20]. Many studies are being taken place following recent growing attention on correlation between tumor immune microenvironment control and cancer treatment [21, 22].

PD-1/PD-L1 ICI drug options should be chosen upon 3P (predictive, preventive, and personalized) medicine concepts because tumor immune microenvironment of patient individuals is varied and fluid. 3P medicine is the best strategy to pursue greater good showing its top-level social maturity for demand of healthy individuals and patient groups, comes with a desirable medical system [23–25].

Tumor immune microenvironment is very complicated that research on finding an adequate biomarker is essential for cultivation of 3P medicine. Efficacious manner to find biomarkers for cancer treatment screening is pattern recognition of molecules such as proteome (or phosphoproteome), dielectric, or metabolome on each patient. Many recent technologies of Omics, statistical biology, and system biology are used on recognition of medicine response molecule patterns in various cancers [26–28].

In this study, new noninvasive biomarker identification is conducted, and its validity is verified through multiple experiment techniques including multi-proteome analysis using blood plasma of PD-1/PD-L1 ICI-treated NSCLC patients which is going to contribute to advancement of medical standard of 3P medicine concepts.

Methods

Reagents and antibodies

Purified rat IgG and anti-PD-1 mAbs were purchased from BioXCell (West Lebanon, NH, USA), and

anti-CD8 β -PE-Cy5 and anti-PD-1-PE antibodies were purchased from BD Bioscience (Franklin Lakes, NJ, USA). TMT11plex reagents used for TMT labeling were purchased from Thermo Fisher Scientific (Waltham, MA, USA). Anti-C7 purified MaxPab antibody (Abnova, Taipei, Taiwan) and goat pAb to Rb IgG (Abcam, Cambridge, UK) antibodies were used for western blotting.

Patients

First, 10 and 53 NSCLC patients who had measurable lesions and received anti-PD-1/PD-L1 immune checkpoint inhibitors from the National Cancer Center (NCC) in Korea were sequentially recruited and enrolled into the test and validation sets, respectively. Next, 99 patients with NSCLC were recruited and assigned into an external validation set for an external retrospective validation study conducted at Samsung Medical Center (SMC) in Korea. All patients in both centers received one of the following drugs until disease progression: nivolumab, pembrolizumab, or atezolizumab. The tumor was assessed using computerized tomography or magnetic resonance imaging every 6 weeks until disease progression. Tumor response was classified according to the Response Evaluation Criteria in Solid Tumor 1.1 [29]. For the test set, approximately 5 mL of whole blood samples was collected before treatment (on day 0) and three times after treatment (on days 7, 14–21, and 40–45). For the validation and external validation sets, samples were collected only before treatment (day 0). Written informed consent was obtained from all patients. This study was approved by the National Cancer Center Institutional Review Board (NCC-2017-0257) and the Samsung Medical Center Institutional Review Board (SMC-2018-04-048).

Blood sample preparation for proteomics analysis

Whole blood samples were collected directly into purple K2-EDTA vacuum tubes (Becton Dickinson) and placed on ice. The plasma tube was centrifuged at 1000 rpm for 15 min at 4 °C within 10 min of collection. From the top of the tube, 0.5 mL of supernatant (plasma) was collected and stored at –80 °C. Forty plasma samples from the training set were depleted according to the manufacturer's instructions using High Select Top 14 abundant protein depletion midi spin columns (Thermo Fisher Scientific, Rockford, IL, USA). The peptide samples were reconstituted in 100 mM triethylammonium bicarbonate (Thermo Fisher Scientific) and labeled using TMT11plex reagents (Thermo Fisher Scientific) according to the manufacturer's instructions.

Liquid chromatography-mass spectrometry/mass spectroscopy analysis (proteomics)

We analyzed 12 TMT-labeled phosphopeptide fractions and 24 global peptide fractions by using a Q Exactive HF-X Hybrid Quadrupole-Orbitrap mass spectrometer (Thermo Fisher Scientific) coupled to the Ultimate 3000 RSLC nano-system (Thermo Fisher Scientific). The peptides were loaded onto a trap column (100 μ m \times 2 cm) packed with Acclaim Pep-Map100 C18 resin (Thermo Fisher Scientific). The loaded peptides were eluted using a gradient of 5 to 36% solvent B (0.1% formic acid in acetonitrile) that was allowed to flow through the column for 180 min at a flow rate of 300 μ L/min. The eluted peptides, separated by an analytical column (EASY-Spray column, 75 μ m \times 50 cm, Thermo Fisher Scientific), were sprayed into a nano-ESI source at an electrospray voltage of 2.3 kV. The Q Exactive HF-X Orbitrap mass analyzer was operated using the top 10 data-dependent methods. Full mass spectroscopy (MS) scans were acquired over the *m/z* 350–2000 range with a mass resolution of 120,000 (at *m/z* 200). The automatic gain control (AGC) target value was 3.00×10^6 . The ten most intense peaks with a charge state ≥ 2 were fragmented in the higher energy collisional dissociation (HCD) collision cell with a normalized collision energy of 32%, and tandem mass spectra were acquired using the Orbitrap mass analyzer with a mass resolution of 45,000 at *m/z* 200.

Database search

All raw data files were searched from the database of Proteome Discoverer 2.3 software (Thermo Fisher Scientific). The SEQUEST-HT and MS Amanda 2.0 programs were used for searching the database against the Swissprot-Human database.

Protein or phosphoprotein abundance ratio

Proteins or phosphoproteins that appeared commonly in the four sample sets (days 0, 7, 14–21, and 40–45) were considered for inclusion in subsequent proteomic or phosphoproteomic analyses. The abundance of each protein or phosphoprotein was expressed as a ratio (abundance ratio = abundance in each sample/abundance in the mixture). The abundance ratio was then converted into common logarithms.

Quantitative analysis of the complement component C7 protein by ELISA

The plasma samples were diluted 200,000-fold using a diluent solution (1 \times TBS, 0.05% Tween-20 with 0.1% BSA, pH

7.2–7.4) and added to an ELISA plate coated with the anti-human complement component 7 (C7) monoclonal antibody (Sino Biological Inc., Beijing, China). All samples were incubated for 2 h at 20–24°C. Then, sample aspiration/washing was performed 3 times, and anti-human C7 polyclonal antibodies conjugated to horseradish peroxidase (Sino Biological Inc.) were added. The reaction mixture was incubated for 1 h at 20–24°C, and aspiration/washing was performed 3 times. Visualization was performed by incubating the reaction mixture with tetramethylbenzidine (TMB) for 20 min, and the color development reaction was stopped by adding a stop solution. The absorbance was measured at 450 nm using a microplate reader (Tecan Sunrise, Tecan, Switzerland).

The MC38 tumor model and antibody treatment

Six- to 8-week-old C57BL/6 mice were purchased from Orient Bio (Gapyeong, Korea). All mice were maintained under specific pathogen-free conditions at the animal facility of the National Cancer Center in Korea. All procedures involving animals were approved by the Institutional Animal Care and Use Committee (IACUC) of the National Cancer Center Institute (NCCI). Female C57BL/6 mice were injected subcutaneously (s.c.), on their backs, with 5×10^5 MC38 tumor cells, and 100 µg of rat IgG or anti-PD-1 mAb was administered every 5 days, from day 10 onwards. The mice were routinely monitored to assess the tumor growth rate.

Flow cytometry

MC38 tumor-bearing mice were treated with rat IgG or anti-4-1BB mAb as described above, and inguinal tumor-draining lymph nodes (TDLNs) were collected from each group of mice on day 18. The single-cell TDLN suspensions were counted with an ADAM-MC2 cell counter (NanoEntek, Seoul, Korea) and stained with anti-CD8β-PE-Cy5 and anti-PD-1-PE. All samples were subsequently analyzed using FACSCalibur (BD Bioscience). The absolute numbers of PD-1+CD8β+ T cells were calculated by multiplying the percentage of measured cells with the total number of viable cells (absolute number = % of measured cells/total cells recovered).

Western blotting analysis of C7

MC38 tumor-bearing mice were treated with rat IgG or anti-4-1BB mAb as described above, and blood was collected from the venous sinus of each group of mice on days 0, 3, 10, 13, and 17. Serum was collected via centrifugation and used to measure C7 levels. To analyze the protein content from the serum, samples were prepared using the IP lysis buffer (Thermo Fisher Scientific) with a complete EDTA-free protease inhibitor tablet (Roche Applied Science, Penzberg,

Germany), LDS sample buffer (Invitrogen, Waltham, MA, USA), and sample reducing agent (Invitrogen). After the heat blocking of the lysates at 70 °C for 10 min, they were incubated on ice for 20 min and cleared via centrifugation at 4 °C for 10 min at 14,000 rpm. Then, the C7 protein was separated from the plasma via electrophoresis on a 4–12% Bis-Tris gel (Invitrogen). The proteins were transferred onto PVDF membranes (Merck Millipore, Burlington, MA, USA), and the presence of C7 was determined using the anti-C7 purified MaxPab (Abnova) antibody and goat pAb to Rb IgG (Abcam) antibody. Protein bands were visualized using enhanced chemiluminescence (ECL) (Thermo Fisher Scientific), and band intensities were analyzed using ImageJ software.

HE staining and immunohistochemistry

MC38 tumor cells were injected into C57BL/6 mice, and rat IgG or anti-4-1BB mAb was administered every 5 days from day 10 after administering the tumor cell injection. Tumor tissues were collected from the mice 3 days after the second injection of Ab was administered and fixed with 10% formalin solution. Fixed tumor tissues were embedded in paraffin wax, and 5-mm sections were cut. Slides were stained with hematoxylin and eosin. Alternatively, the sections were stained with anti-C7 mAb (Abcam), stained with HRP-conjugated secondary Ab, colored with DAB chromogen, and counter-stained with hematoxylin.

Statistical analysis

Regardless of the sampling time, quantitative comparison analysis was performed using one-way ANOVA and Pearson's correlation analysis. Another quantitative comparison analysis between the sampling time periods was performed using the StandardScaler function in the scikit learn module, along with one-way ANOVA, and multiple comparison tests. Tukey's HSD module was used for post hoc analysis in the stasmodel module (v0.11.0dev0, <http://www.statsmodels.org/>) coded into an in-house program (Python 2.7). The correlation analyses of key proteins were performed using R software version 3.5.3, and a two-sided *p* value of less than 0.05 was considered to be indicative of statistical significance. An area under the curve (AUC) was used to evaluate the single summary measure of diagnosis performance using the non-parametric trapezoidal method. All analyses were performed using the IBM® SPSS® software. Correlation analyses involving the major proteins, accuracy (ACC), and receiver operating characteristic (ROC) were considered statistically significant. A two-tailed *p* value of less than 0.05 was considered statistically significant.

Results

Patients

A total of 162 non-small cell lung cancer patients were recruited for this study through two other centers, the National Cancer Center (NCC) ($N = 63$) and Samsung Medical Center (SMC) ($N = 99$) in Korea (Table 1). Patients at the NCC were classified into a training set ($n = 10$) and validation set ($n = 53$), and all patients at SMC were assigned to an external validation set. The median age of patients in both centers was 64.4 years, and approximately 80% of the patients were male. Based on the results of the analysis performed using RECIST V1.1., patients were classified as complete responders (CR) and partial responders (PR), or as those with stable disease (SD) or progressive disease (PD). In NCC, PR (34.9%) and SD patients (7.9%) with a PFS \geq 6 months were classified into the group of responders with clinical benefits. Conversely, SD (15.9%) and PD (41.3%)

patients with a PFS of < 6 months were classified as non-responders without clinical benefits. For SMC, CR (2%), PR (38.4%), and SD (16.2%) patients were classified as responders, and SD (14.1%) and PD (29.3%) patients were classified as non-responders. Adenocarcinoma (ADC), squamous cell carcinoma (SqCC), and other NSCLC patients were classified according to their histological type; more than half of the patients in both centers had ADC NSCLC. Patients who were treated with one of the three types of PD-1/PD-L1 immunotherapy agents, i.e., atezolizumab (Ate), nivolumab (Niv), and pembrolizumab (Pem), were recruited, and most patients were treated with Pem. The smallest number of patients was treated with Niv in both centers. The patients were evaluated using 22C3 or SP263 companion diagnostic (CDx) assays; in NCC, 27 and 58 patients were evaluated using the 22C3 CDx and SP263 CDx assays, respectively. In SMC, 93 and 80 patients were evaluated with 22C3 and SP263 CDx assays, respectively.

Table 1 Characteristics of patients participating in a study for the development of new diagnostics that could predict the response of PD-L1 immune checkpoint inhibitors

Clinical characteristics	NCC ($N = 63$)	SMC ($N = 99$)	Total ($N = 162$)
Median age (range), years	64.4 (37.0–85.0)	64.4 (32.0–82.0)	64.4 (32.0–85.0)
Sex, N (%)			
Male	50 (79.4)	86 (86.9)	136 (84.0)
Female	13 (20.6)	13 (13.1)	26 (16.0)
Set, N (%)			
Training set	10 (15.9)		10 (6.2)
Validation set	53 (84.1)		53 (32.7)
External validation set		99 (100)	99 (61.1)
Response, N (%)			
CR		2 (2)	2 (1.2)
PR	22 (34.9)	38 (38.4)	60 (37.0)
SD (Responder)	5 (7.9)	16 (16.2)	21 (13.0)
SD (Non-responder)	10 (15.9)	14 (14.1)	24 (14.8)
PD	26 (41.3)	29 (29.3)	55 (34.0)
NSCLC histology, N (%)			
ADC	38 (60.3)	53 (53.6)	91 (56.1)
SqCC	19 (30.2)	33 (33.3)	52 (32.0)
Other	6 (9.5)	13 (13.1)	19 (11.7)
PD-1/PD-L1 immunotherapy, N (%)			
Pembrolizumab	26 (41.3)	53 (53.6)	79 (48.8)
Nivolumab	18 (28.6)	12 (12.1)	30 (18.5)
Atezolizumab	19 (30.2)	34 (34.3)	53 (32.7)
PD-1/PD-L1 CDx, N (%)			
22C3	27 (42.9)	93 (94.0)	120 (74.1)
SP263	58 (92.1)	80 (80.8)	138 (85.2)

NCC, National Cancer Center; SMC, Samsung Medical Center; N , number; CR, complete response; PR, partial response; SD, stable disease; PD, progressive disease; responder, responder with clinical benefit (PFS \geq 6 months); Non-responder, non-responder without clinical benefit (PFS $<$ 6 months); NSCLC, non-small-cell lung cancer; ADC, adenocarcinoma; SqCC, squamous cell carcinoma; Other, other histological types of NSCLC; CDx, companion diagnostic

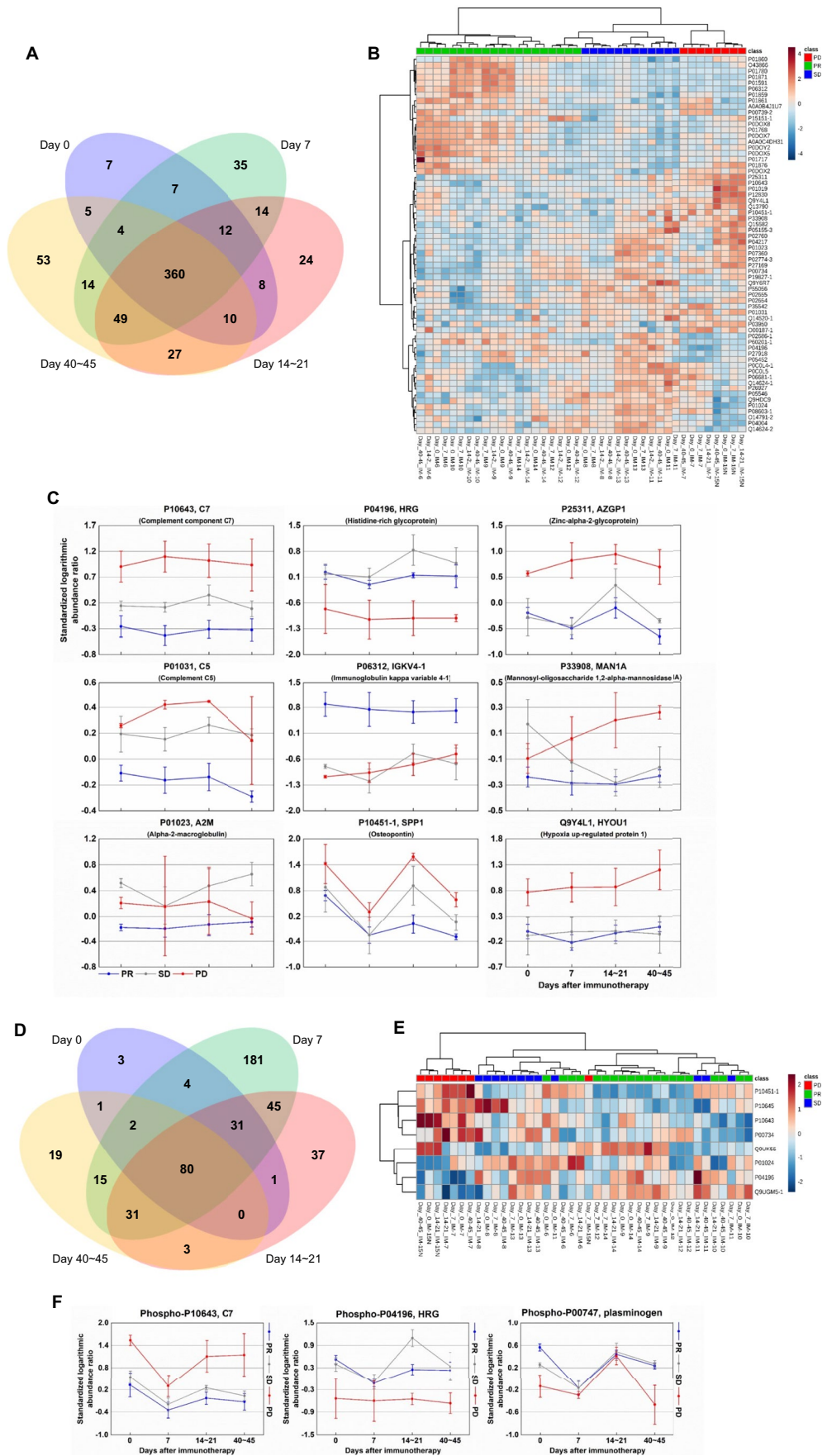


Fig. 1 Proteomic analysis of blood plasma obtained from NSCLC patients. **A** Venn diagram showing the overlap of proteins measured individually according to the sampling schedule. **B** A heatmap of hierarchical clusters between the PR, SD, and PD sample groups with 64 proteins, with a p value < 0.05 . PR (green), partial response; SD (blue), stable disease; PD (red), progressive disease. **C** Result of the ANOVA and post hoc (Tukey's HSD) analyses during the sampling period, during days 0, 7, 14–21, and 40–45. Differences were observed for a total of 9 proteins between the PR, SD, and PD groups, and the p value was < 0.05 on at least 2 sampling days, compared to the training set. The results are expressed as mean \pm SEM values. **D** Venn diagram showing the overlap between phosphoproteins whose levels were measured individually according to the sampling schedule. **E** A heatmap showing the hierarchical clustering between the PR, SD, and PD sample groups with 8 phosphoproteins, with a p value < 0.05 (right). PR (green), partial response; SD (blue), stable disease; PD (red), progressive disease. **F** Results of the ANOVA and post hoc (Tukey's HSD) analysis during each of the 4 sampling periods on days 0, 7, 14–21, and 40–45. Differences were observed in the levels of 3 phosphoproteins between the PR, SD, and PD groups, and the p value was < 0.05 on 2 sampling days, compared to the training set. Phospho-P10643; phospho-P04196; and phospho-P00747. The results were expressed as mean \pm SEM values. P10643, complement component C7; P01031, complement C5; P01023, alpha-2-macroglobulin; P04196, histidine-rich glycoprotein; P06312, immunoglobulin kappa variable 4-1; P10451-1, osteopontin; P25311, zinc-alpha-2-glycoprotein; P33908, mannosyl-oligosaccharide 1,2-alpha-mannosidase IA; and Q9Y4L1, hypoxia up-regulated protein 1

Discovery of protein candidates for predicting the response to the PD-1/PD-L1 immune checkpoint inhibitor in NSCLC patients

To discover new biomarkers that could compensate for the shortcomings of the current PD-1/PD-L1 immune checkpoint inhibitor (ICI) CDx, we performed an analysis using plasma obtained from NSCLC patients by a noninvasive method. We expected that the quantitative difference in specific proteins in the patient's blood would affect the responsiveness to PD-1/PD-L1 ICI. In addition, it was thought that the quantitative change in a specific protein would also appear, depending on the frequency of PD-1/PD-L1 ICI treatment. To prove this, blood samples were collected from 10 patients in the training set at NCC. Blood was collected from each patient before (day 0) and after the first (day 7), second (day 14–21), and third (day 40–54) treatments. The relative levels of various proteins were then analyzed and compared according to the RECIST V1.1–based method for response classification.

As shown in the Venn diagram (Fig. 1A), levels of 360 proteins were simultaneously measured in the four sample groups (S1 Table), and quantitative comparative methods were used to identify protein candidates that could discriminate between the PR, SD, and PD groups. Distinct differences were observed for a total of 25 out of the 360 proteins between the PR, SD, and PD groups ($p < 0.05$; Fig. 1B and S2 Table), of which nine proteins, i.e., P10643(C7), P01031

(C5), P01023 (A2M), P04196 (HRG), P06312 (IGKV4-1), P10451-1 (osteopontin), P25311 (AZGP1), P33908 (MAN1A1), and Q9Y4L1 (HYOU1), showed distinctly different patterns on two or more sampling days (Fig. 1C; S3 Table).

Furthermore, to determine the correlation between protein activation and response to PD-1/PD-L1 ICI treatment, the level of phosphorylated protein, an activated form of the protein, was determined. Eighty phosphoproteins were simultaneously measured in four sample groups, and their relative quantification was calculated (Fig. 1D; S1 Table). As a result of the analysis, eight phosphoproteins were classified as proteins that could discriminate between the PR, SD, and PD groups; the p value was < 0.05 (Fig. 1E; S2 Table). Of these eight proteins, distinct differences were observed for three phosphoproteins, i.e., phospho-C7 (P10643), phospho-HRG (P04196), and phospho-plasminogen (P00747), between the two sample groups on different sampling days (Fig. 1F; S3 Table). Interestingly, it was confirmed that the amounts of plasma C7 and HRG were relatively different in the PR, SD, and PD groups during both total protein and phosphoprotein analysis, and that these differences persisted regardless of the sampling time. Based on these results, plasma C7 and HRG were selected as the most ideal candidate biomarkers that could predict responses to PD-1/PD-L1 ICIs in NSCLC patients.

Evaluation of the efficacy of plasma C7 as a biomarker for predicting the response of PD-1/PD-L1 ICI through a multi-center analysis

Next, we aimed to confirm whether C7 and HRG, the candidate biomarkers identified by the proteomics approach, could be used as diagnostic tools. The concentrations of C7 and HRG were measured in 31 NSCLC patients at NCC by using ELISA. To confirm the ability of C7 and HRG to discriminate between responders and non-responders, receiver operating characteristic (ROC) analysis was performed using each measured concentration value. The AUC (area under the ROC curve) for C7 was 0.949 (95% CI, 0.867–1.030), whereas it was 0.633 (95% CI, 0.436–0.829) for HRG (S1 Fig). These results were in contrast to those obtained with proteomics analysis, since an excellent AUC value was observed only for C7, and the subsequent study focused on the C7 quantified through ELISA.

To confirm the feasibility of using the biomarker plasma C7 as a novel CDx for PD-1/PD-L1 ICIs, we included 53 NSCLC patients into the validation set at NCC. A total of 63 NSCLC patients were designated as the NCC set for follow-up studies. In addition, to ensure that plasma C7 could be reliably used as a biomarker, a multi-center retrospective study was conducted at a contract research organization (CRO) at SMC that was monitored by a clinical

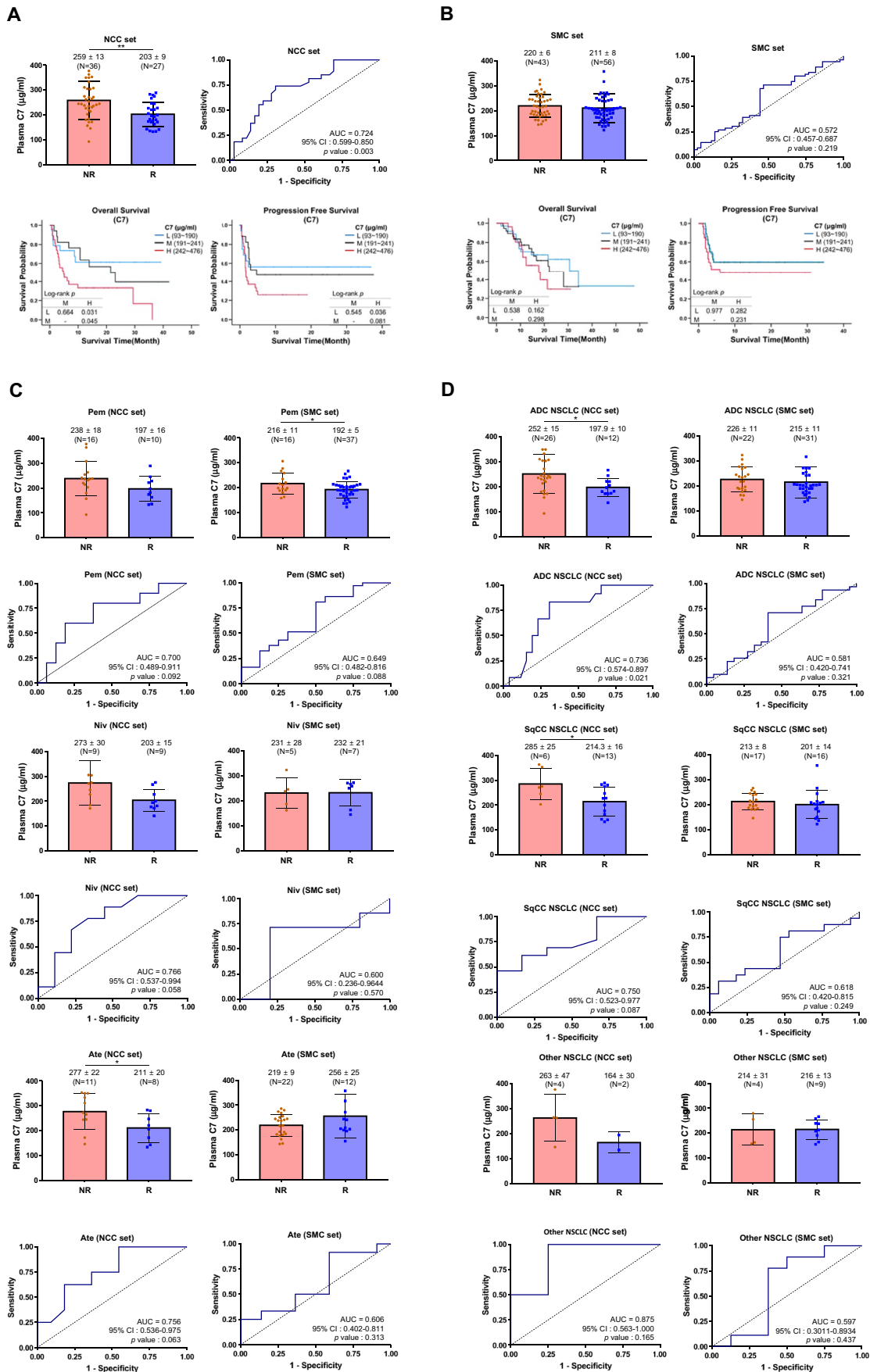


Fig. 2 Distribution of plasma C7 concentrations in patients recruited from NCC and SMC. **A** Plasma C7 analysis of all patients in the NCC set, and distribution of the C7 concentration values (upper left), ROC analysis using C7 concentration values (upper right), analysis of OS according to C7 concentration distribution (lower left), and analysis of PFS according to C7 concentration distribution (lower right). **B** Plasma C7 analysis of all patients in the SMC set, and distribution of C7 concentration values (upper left), ROC analysis using C7 concentration values (upper right), analysis of OS according to C7 concentration distribution (lower left), and analysis of PFS according to C7 concentration distribution (lower right). **C** Analysis of plasma C7 distribution according to PD-1/PD-L1 immunotherapy type in the NCC (left) and SMC set (right), and ROC analysis using C7 concentration values. **D** Analysis of plasma C7 distribution according to NSCLC histology type in the NCC (left) and SMC set (right), and ROC analysis using C7 concentration values. The C7 concentration values were expressed as mean \pm SD values (* $p < 0.05$; ** $p < 0.01$; *** $p < 0.005$). NCC, National Cancer Center; SMC, Samsung Medical Center; NR, non-responder group; R, responder group; L, low; M, medium; H, high; Pem, pembrolizumab; Niv, nivolumab; Ate, atezolizumab; NSCLC, non-small cell lung cancer; ADC, adenocarcinoma; SqCC, squamous cancer cell; OS, overall survival; PFS, progression-free survival

research associate (CRA) at Synex Consulting in Korea. Samples from 99 NSCLC patients recruited from the SMC into the external validation set were assigned to the SMC set, and a follow-up study was conducted.

First, by analyzing the C7 concentrations in the NCC set, it was confirmed that the mean concentration of C7 for PD-1/PD-L1 ICI was significantly lower in the responder group than in the non-responder group (Fig. 2A). The AUC for the NCC set was determined to be 0.724 (95% CI, 0.599–0.850) via ROC analysis, indicating that the diagnostic method was used effectively (Fig. 2A). Additionally, the range of C7 concentration values of patients was classified as low (93–190 $\mu\text{g}/\text{mL}$), medium (191–241 $\mu\text{g}/\text{mL}$), and high (242–476 $\mu\text{g}/\text{mL}$), and it was confirmed that there were changes in the overall survival (OS) and progression-free survival (PFS) according to the C7 concentration values. As a result, it was confirmed that the OS and PFS of patients with low C7 concentrations were significantly higher than those of patients with high C7 concentrations (Fig. 2A).

As a next step, plasma C7 concentration values were measured in SMC set which showed no significant differences between the responder group and non-responder group (Fig. 2B). The AUC of plasma C7 in the SMC set was found to be 0.572 (95% CI, 0.457–0.687) through ROC analysis. Upon analyzing the OS and PFS of patients by their C7 levels, it was confirmed that the OS and PFS of patients with low C7 concentrations were slightly higher than those of patients with high C7 concentrations. Although the trends of the NCC and SMC sets were similar, the analytical performance of C7 as a biomarker was better in the NCC set than in the SMC set.

Analysis of target NSCLC patients in plasma C7 as a biomarker for predicting the response to PD-1/PD-L1 ICIs through a multi-center analysis

The utility of the diagnostic method using the selected biomarker plasma C7 was confirmed in the NCC set but appeared to be less useful in the SMC set. However, it was expected that the usefulness of plasma C7 as a biomarker would vary according to the type of PD-1/PD-L1 immunotherapy treatment and NSCLC histology. After PD-1/PD-L1 immunotherapy and NSCLC histology classification of NSCLC patients from the NCC and SMC sets, the C7 concentration distribution and AUC were confirmed. As observed with the previous results, in the NCC set, it was confirmed that the average concentration of C7 in the responder group was lower than that of the non-responder group in all PD-1/PD-L1 immunotherapy groups, including pembrolizumab, nivolumab, and atezolizumab groups (Fig 2C, left line). It was also confirmed that the average concentration of C7 was lower in the responders of all NSCLC histology groups, including ADC, SqCC, and other groups, than in the non-responders (Fig 2D, left line). Furthermore, the AUC was greater than 0.7 in all groups of the NCC set. In the SMC set, only the pembrolizumab group had a significantly lower C7 concentration in the responder group than in the non-responder group. In addition, the AUC of C7 in the pembrolizumab group was 0.649, which was higher than that of the other groups (Fig 2C, right line).

Next, an analysis was conducted to set a cutoff value for utilizing plasma C7 as a diagnostic method in the field. Sensitivity (SEN) and specificity (SPE) were calculated based on the temporal cutoff values obtained through the preceding ROC analysis. Among the following temporal cutoff values, those that yielded Youden's J statistic values of 0.2 or greater were selected as candidate cutoffs (S4 Table) [30]. Then, the positive predictive value (PPV), negative predictive value (NPV), and accuracy (ACC) for the candidate cutoff were further analyzed. The ideal cutoff concentration for the NCC set was 230 $\mu\text{g}/\text{mL}$, and the ideal cutoff concentration for the SMC set was calculated to be 215 $\mu\text{g}/\text{mL}$. After classifying patients with NCC and SMC sets in the same manner as before, the ability to discriminate PD-1/PD-L1 ICI responses was analyzed based on selected plasma C7 cutoff concentrations. The analytical performance of ACC in the total patients in the NCC and SMC sets was 70.4% and 63.6%, respectively (Table 2).

The ability to discriminate the reactivity of plasma C7 according to each immunotherapy method was investigated. The AAC of plasma C7 for the pembrolizumab group in the SMC set was 73.6%, which was similar to that of the pembrolizumab group (73.7%) in the NCC group (Table 2). However, the AAC of plasma C7 in all groups except the pembrolizumab group of the SMC set was lower than that

Table 2 Analytical performance evaluation of plasma C7 for predicting the response to PD-1/PD-L1 ICIs

	SEN	SPE	PPV	NPV	ACC
NCC set					
Total patients	74.1 (20/27)	69.4 (25/36)	64.5 (20/31)	78.1 (25/32)	70.4
Type of immunotherapy					
Pembrolizumab	62.5 (5/8)	80.8 (9/11)	70.4 (5/7)	75.0 (9/12)	73.7
Nivolumab	77.8 (7/9)	66.7 (6/9)	70.0 (7/10)	75.0 (6/8)	72.2
Atezolizumab	80.0 (8/10)	62.5 (10/16)	57.1 (8/14)	83.3 (10/12)	69.2
Type of histology					
ADC NSCLC	83.3 (10/12)	65.4 (17/26)	52.6 (10/19)	89.5 (17/19)	70.1
SqCC NSCLC	60.5 (8/13)	83.3 (5/6)	88.9 (8/9)	50.0 (5/10)	68.4
Other NSCLC	100.0 (2/2)	75.0 (3/4)	66.7 (2/3)	100.0 (3/3)	83.3
SMC set					
Total patients	70.4 (40/56)	53.5 (23/43)	66.7 (40/60)	59.0 (23/39)	63.6
Type of immunotherapy					
Pembrolizumab	86.5 (32/37)	43.8 (7/16)	78.0 (32/41)	58.3 (7/12)	73.6
Nivolumab	28.6 (2/7)	60.0 (3/5)	50.0 (2/4)	37.5 (3/8)	40.7
Atezolizumab	50.0 (6/12)	59.1 (13/22)	40.0 (6/15)	68.4 (13/19)	55.9
Type of histology					
ADC NSCLC	70.0 (22/31)	59.1 (13/22)	70.0 (22/31)	59.1 (13/22)	66.0
SqCC NSCLC	80.3 (13/16)	47.1 (8/17)	59.1 (13/22)	72.7 (8/11)	63.6
Other NSCLC	55.6 (5/9)	50.0 (2/4)	70.4 (5/7)	33.3 (2/6)	53.8

SEN, sensitivity; SPE, specificity; PPV, positive predictive value; NPV, negative predictive value; ACC, accuracy. Values are presented as percentage values (actual patient number/total patient number)

of the NCC set (Table 2). Results derived from the other two centers showed that plasma C7 could be specifically applied as a biomarker for predicting the reactivity to pembrolizumab immunotherapy.

Comparative evaluation of current companion diagnostics (22C3 and SP263) and plasma C7 to predict the response of pembrolizumab

To verify the efficacy of plasma C7, the ability to predict the response of pembrolizumab as an FDA- or CE-approved CDx (22C3 and SP263) and the predictive ability of C7 were compared. This comparative analysis was performed on all patients from the other two centers.

First, the distribution of the PD-L1 tumor proportion score (TPS) of patients treated with pembrolizumab in both responders and non-responders was confirmed. It was confirmed that the PD-L1-stained TPS with 22C3 and sp263 was more than 50% in the responder group and less than 50% in the non-responder group (Fig. 3A and B).

The mean C7 concentration in the responder group of all patients treated with pembrolizumab was significantly lower than that in the non-responder group (Fig. 3C). Next, upon comparing AUC values, the AUC of C7 was found to be higher than that of 22C3 and SP263 (Fig. 3A–D). In addition, OS and PFS, in terms of TPS %, for the current CDx and C7 concentrations were determined; the OS and PFS were significantly

higher when the PD-L1 TPS was 50% or higher, as compared to when it was less than 50%. Patients with low C7 concentrations had significantly longer OS and PFS than those with high C7 concentrations.

To compare the analytical performance, the two cutoff TPS % (≥ 1 , ≥ 50) of 22C3 and SP263, and the selected plasma C7 cutoff concentrations were used to compare the predictive accuracy. For the total number of patients in the 22C3 group, the ACC of 22C3 CDx ranged from 64.1 to 70.3%, and the plasma C7 was 71.9% (Table 3).

In the SP263 group, the ACC of plasma C7 detection was 68.2%, and for SP263, the ACC was distributed between 60.6 and 62.1%. Moreover, the prediction accuracy of C7 for the response to pembrolizumab was higher than that of conventional CDx in both the NCC and SMC sets.

These results suggest that plasma C7 can sufficiently serve as a substitute for current CDx that were used for predicting the response to pembrolizumab.

Plasma C7 as an adjunct to current companion diagnostic (22C3 and SP263) methods for predicting response to pembrolizumab

Therefore, we conducted an additional analysis to determine the role of C7 as an adjunct that could compensate for the shortcomings of the current CDx. To confirm the correlation between the PD-L1 TPS % and C7 concentration

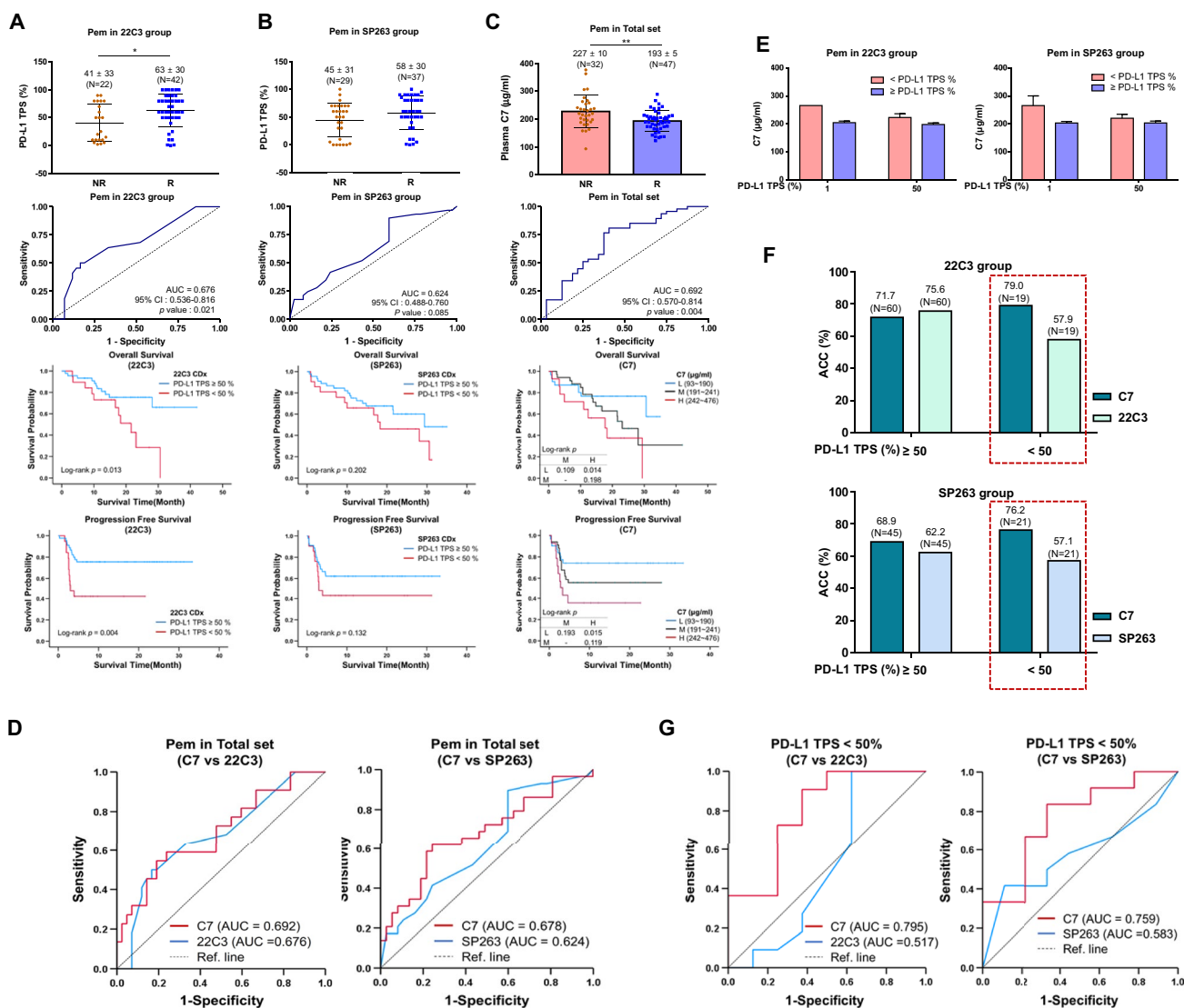


Fig. 3 Analytical performance evaluation of pembrolizumab-treated patients. **A** Distribution of PD-L1 TPS of 22C3, a CDx for pembrolizumab; ROC analysis, OS analysis according to 22C3 TPS %, and PFS analysis according to 22C3 TPS %. **B** Distribution of PD-L1 TPS of SP263, a CDx for pembrolizumab; ROC analysis, OS analysis according to SP263 TPS %, and PFS analysis according to SP263 TPS %. **C** Distribution of plasma C7 concentration values, ROC analysis, OS analysis according to C7 concentration values, and PFS analysis according to C7 concentration values. **D** Comparative analysis of ROC of pembrolizumab CDx 22C3 and plasma C7 (left). Comparative analysis of ROC values for pembrolizumab CDx SP263 and plasma C7 (right). **E** Distribution of C7 concentration val-

ues according to the PD-L1 TPS % cutoff; classification according to 22C3 (left) and SP263 (right). **F** Accuracy analysis of 22C3, SP263, and plasma C7 in patients with a PD-L1 TPS of ≥ 50% when < 50% of patients were treated with pembrolizumab. Classification according to 22C3 (upper) and SP263 (lower). **G** ROC analysis of 22C3, SP263, and plasma C7 in patients with a PD-L1 TPS of < 50% who were treated with pembrolizumab. Comparison of C7 vs 22C3 (left) and C7 vs SP263 (right). The results of **A**, **B**, and **C** were expressed as mean ± SD values (*p < 0.05; **p < 0.01; ***p < 0.005). NR, non-responder group; R, responder group; Pem, pembrolizumab; OS, overall survival; PFS, progression-free survival; TPS, tumor proportion score; ACC, accuracy; Ref. line, reference line

distribution, the concentration of C7 was confirmed by distinguishing between 22C3 and SP263 PD-L1 at values above or below the TPS % cutoff. Interestingly, the group expected to be a responder according to the TPS % cutoff had a lower C7 concentration (Fig. 3E).

In the case of conventional CDx, the prediction accuracy of the response to pembrolizumab for patients with a TPS

> 50% was 75.6% and 62.2% for 22C3 and SP263, respectively (Fig. 3F). However, for patients with a TPS < 50%, the prediction accuracy of 22C3 and SP263 was very low, i.e., approximately 57%. However, in the case of C7, even with a TPS < 50%, the response prediction accuracy was more than 75%, and the AUC was also confirmed to be ≥

Table 3 Comparative analysis of plasma C7 and current CDx (SP263 and 22C3) markers with regard to their discriminant predictive performance for determining the response to pembrolizumab

	Diagnostic method	Cutoff	SEN	SPE	PPV	NPV	ACC
22C3 group							
NCC	C7 (µg/mL)	≤ 230	83.3 (5/6)	83.3 (5/6)	83.3 (5/6)	83.3 (5/6)	83.3
	22C3 (TPS %)	≥ 1	100.0 (6/6)	0.0 (0/6)	50.0 (6/12)	N/A	50.0
SMC	C7 (µg/ml)	≥ 50	83.3 (5/6)	50.0 (3/6)	62.5 (5/8)	75.0 (3/4)	66.7
		≤ 215	86.1 (31/36)	43.8 (7/16)	77.5 (31/40)	58.3 (7/12)	73.1
	22C3 (TPS %)	≥ 1	97.2 (35/36)	0.0 (0/16)	68.6 (35/51)	0.0 (0/1)	67.3
Total	C7 (µg/ml)	≥ 50	80.6 (29/36)	50.0 (8/16)	78.4 (29/37)	53.3 (8/15)	71.2
		≤ 215	81.0 (34/42)	54.5 (12/22)	77.3 (34/44)	60.0 (12/20)	71.9
	22C3 (TPS %)	≥ 1	97.6 (41/42)	0.0 (0/22)	65.1 (41/63)	0.0 (0/1)	64.1
		≥ 50	78.6 (33/42)	54.5 (12/22)	76.7 (33/43)	57.1 (12/21)	70.3
SP263 group							
NCC	C7 (µg/ml)	≤ 230	77.8 (7/9)	57.1 (8/14)	53.8 (7/13)	80.0 (8/10)	65.2
	SP263 (TPS %)	≥ 1	100.0 (9/9)	14.3 (2/14)	42.9 (9/21)	100.0 (2/2)	47.8
SMC	C7 (µg/ml)	≥ 50	88.9 (8/9)	21.4 (3/14)	42.1 (8/19)	75.0 (3/4)	47.8
		≤ 215	82.1 (23/28)	46.7 (7/15)	74.2 (23/31)	58.3 (7/12)	69.8
	SP263 (TPS %)	≥ 1	96.4 (27/28)	20.0 (3/15)	69.2 (27/39)	75.0 (3/4)	69.8
Total	C7 (µg/ml)	≥ 50	71.4 (20/28)	60.0 (9/15)	76.9 (20/26)	52.9 (9/17)	67.4
		≤ 215	78.4 (29/37)	55.2 (16/29)	69.0 (29/42)	66.7 (16/24)	68.2
	SP263 (TPS %)	≥ 1	97.3 (36/37)	17.2 (5/29)	60.0 (36/60)	83.3 (5/6)	62.1
		≥ 50	75.7 (28/37)	41.4 (12/29)	62.2 (28/45)	57.1 (12/21)	60.6

Pem, pembrolizumab; *SEN*, sensitivity; *SPE*, specificity; *PPV*, positive predictive value; *NPV*, negative predictive value; *ACC*, accuracy; *TPS*, tumor proportion score. Values are presented as percentage values (actual patient number/total patient number)

0.7, which confirmed that it was more accurate than the 22C3 and SP263 CDx (Fig. 3G).

Thus, patients with a TPS of < 50% upon primary staining with PD-1/PD-L1 CDx could be assessed using plasma C7 to predict the response to pembrolizumab. Our results suggest that the accuracy of this novel method was significantly greater than that of the current PD-1/PD-L1 CDx.

PD-1 blockade suppresses MC38 tumor growth and accompanies the accumulation of complement C7 in tumor tissues via the consumption of C7 in the blood

Our current data indicated that the complement C7 level in the blood plasma was low in patients exhibiting a good oncologic response to PD-1 ICIs (Fig. 2). Although the complement system is known to have regulatory roles in cancer immunity, as it is involved in the inhibition of anti-tumor T cell responses via C3aR- or C5aR1-mediated recruitment and/or activation of immune-suppressive cells, the complement system generally enhances anti-tumor immunity through either complement-dependent cytotoxicity (CDC) or antibody-dependent cellular cytotoxicity (ADCC). Since both CDC and ADCC require the generation of enhanced humoral responses, particularly against tumor cells, and the PD-1 blockade enhances humoral responses, we hypothesized that the decrease in the blood C7 level may be the

result of enhanced consumption of complement components in the tumor tissues. Therefore, we routinely injected rat IgG or anti-PD-1 mAb into the MC38 tumor-bearing B6 mice, as described in Fig. 4A, and monitored the tumor growth rate and the C7 level in blood and tumor tissues.

The PD-1 blockade significantly suppressed the growth of MC38 tumor cells (Fig. 4B) and increased the total number of PD-1⁺CD8⁺ T cells in inguinal TDLN cells on day 18 (Fig. 4C). Consequently, lymphocyte infiltration into the tumor tissues was enhanced in the anti-PD-1-treated mice, compared to that in the rat IgG-treated mice (Fig. 4D).

To monitor the C7 level in the blood, blood samples were routinely collected from rat IgG- or anti-PD-1-treated mice. The blood C7 concentration tended to gradually increase in rat IgG-treated mice, indicating that the inflammation induced by tumor growth promoted C7 production. It was sharply and significantly decreased following treatment with the anti-PD-1 mAb (Fig. 4E). As expected, when the paraffin sections of tumor tissues obtained on day 18 were stained with anti-C7 mAb, the extent of C7 deposition was enhanced in the tumor cells of anti-PD-1-treated mice, compared to that of rat IgG-treated mice (Fig. 4F). These data suggest that tumor growth increased the C7 level in the blood, and the PD-1 blockade enhanced the deposition of C7 in the tumor tissues, probably via the consumption of C7 in the blood.

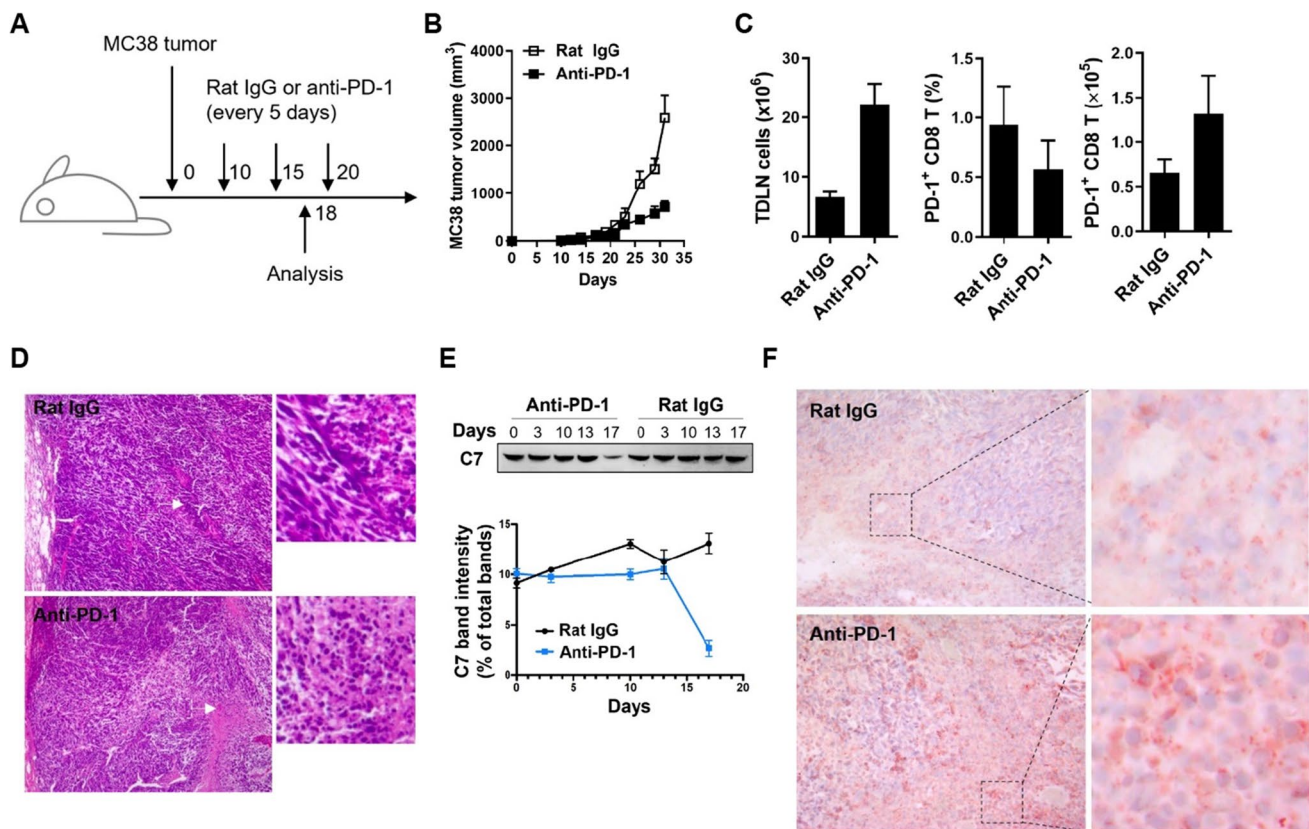


Fig. 4 PD-1 blockade enhances the deposition of C7 in the tumor tissues. **A** Experimental scheme for the MC38 tumor challenge and Ab treatment. **B** The MC38 tumor growth rate of rat IgG- or anti-PD-1-treated mice. **C** Numbers of TDLN cells as well as the percentages and numbers of the PD-1⁺CD8⁺ T cells in the inguinal TDLNs on day 18. **D** H&E staining of the tumor tissues on day 18. **E** Western

blot analysis of C7 in the serum. **F** The C7 IHC of rat IgG- or anti-PD-1-treated tumor tissues on day 18. Data for two (**C–F**) or three (**B**) independent experiments with 5 mice (**B, C**) or 3 mice (**D–F**) per experiment are shown. The Student *t* test was performed in **C** and **E**, and results are shown as mean \pm SD values ($*p < 0.05$; $**p < 0.01$; $***p < 0.005$)

Discussion

A typical shortcoming when treating PD-1/PD-L1 antibody-mediated companion diagnostic (CDx) is chance of miss prescription caused by failed immune checkpoint inhibitor (ICI) response prediction which ends up aggravating NSCLC patients. This is opposite to predictive, preventive, and personalized (3P) medicine, the valued concept in modern medical science. Hence, in order to achieve efficient PD-1/PD-L1 ICI treatment, novel, cost-effective, and noninvasive CDx in 3P medicine perspective is needed.

Identification of plasma proteins to predict PD-1/PD-L1 ICI response

Hence, we first analyzed the plasma of ten NSCLC patients from the training set at NCC by using the multi-omics method to discover new biomarkers; nine key proteins and three key phosphoproteins were identified (Fig. 1). Of these, only plasma C7 and HRG were relatively different between the PR, SD, and PD

groups in both total protein and phosphoprotein analyses. ROC analysis was performed on the responder and non-responder groups by quantitatively measuring the plasma C7 and HRG levels in thirty-one patients in the NCC set (S1 Fig). In contrast to the results of proteomics analysis, an excellent AUC value was observed upon analyzing only the plasma C7 levels. Hence, the subsequent study focused on the assessment of plasma C7 levels. In addition, complement component 5 (C5), which plays a major role in the formation of the complement membrane attack complex in the complement system, was also included among the identified candidate biomarkers. Unexpectedly, the quantitative plasma C5 and C7 patterns analyzed by ELISA were completely different. It could be inferred that this was attributable to a new, independent role of plasma C7 (S1 Fig).

Multi-center validation of plasma C7 as a predictive biomarker for PD-1/PD-L1 ICI response

To examine the usefulness of the diagnostic method involving the use of plasma C7 as the selected biomarker, ROC

analyses of the predictions for the responder and non-responder groups were performed using the plasma C7 concentration values of the NCC set, to select the ideal cutoff concentration value. The ACC determined from the plasma C7 cutoff value of 230 $\mu\text{g/mL}$ for the NCC set was 71.4%, and was higher than that observed with cutoff values for other candidates (S4 Table). Hence, we hypothesized that plasma C7 could be used as a predictive tool to assess reactivity to PD-1/PD-L1 immunotherapy.

A retrospective external validation was conducted at the SMC to ensure the reliability of using plasma C7 as a biomarker. The ROC analysis for plasma C7 was performed in the same manner as in the previous experiment, but an ideal cutoff of 215 $\mu\text{g/mL}$ was identified for the SMC set (S4 Table). Although the selected ideal cutoffs from the NCC and SMC sets were different, a cutoff value of 215 $\mu\text{g/mL}$ was observed to be associated with an ACC of 68.3%, from among the cutoff candidates in the NCC set (S4 Table). Since the cutoff value is affected by the difference in the plasma C7 concentrations in the patients, there would be some differences in each specific group. However, we believe that these differences will be resolved naturally through follow-up studies involving a larger number of patients. In contrast to our expectations, the ACC of plasma C7 in the SMC set was approximately 8% lower than that in the NCC set. Additionally, the ACC for each group in the SMC set was reduced by 5 to 30%, compared to the ACC for the NCC set (Table 2).

These different results are thought to be attributable to the difference in the ratio of responders and non-responders or the PD-L1 TPS % distribution ratio of patients included in each group from the NCC and SMC sets. On the other hand, the accuracy with which plasma C7 could predict the response to pembrolizumab in the NCC and SMC sets was similar, regardless of the proportion of patients with specific disease types. Therefore, we hypothesized that plasma C7 could predict the response to pembrolizumab in all NSCLC patients without its use being limited to specific patients.

Comparison of plasma C7 with current CDx (22C3 and SP263) methods

Currently, in Korea, PD-1/PD-L1 ICI is not approved as a first-line treatment; thus, only patients receiving PD-1/PD-L1 immunotherapy as the second-line treatment were included in this study. The cutoff values of 22C3 and SP263 CDx, which determine whether PD-1/PD-L1 ICIs could be administered as the second-line treatment, mainly have a TPS $\geq 1\%$. [11] However, since the standard of the current CDx marker may be revised through various clinical trials, the ACC of the CDx was calculated using various cutoff TPS % values, including 1% and 50%, regardless of whether PD-1/PD-L1 ICIs were administered as the

first-line or second-line treatment. A comparative analysis of the AUC and ACC values of plasma C7 with those for 22C3 and SP263 CDx in the NCC set showed that predictions performed using the plasma C7 concentration were more accurate than those observed with 22C3 and SP263 for each immunotherapy and NSCLC histology group (S5 and S6 Tables). Contrary to our expectations, the AUC of plasma C7 was slightly higher than that observed for the 22C3 and SP263 CDx assays in the pembrolizumab group of the SMC set alone (S5 Table). Based on these results, it was hypothesized that the most ideal target group for plasma C7 would be the patient group for which pembrolizumab treatment is required.

Plasma C7 as an adjuvant for 22C3 and SP263 methods

Therefore, we studied the role of plasma C7 not only as a new substitute but also as a complement to the current CDx. We have shown that a combination of diagnostic methods using current PD-1/PD-L1 CDx and plasma C7 could complement the low accuracy of the current method. The most important consideration while determining this combination is to select an appropriate cutoff value for plasma C7 level. In this study, a cutoff of 215 $\mu\text{g/mL}$ was selected by performing ROC analysis using the C7 concentration of patients with 22C3 and SP263 TPS values of $\geq 50\%$, and a cutoff of 187 $\mu\text{g/mL}$ was selected for patients with 22C3 and SP263 TPS values of less than 50% (S7 Table). Since the diagnostic cutoff value is different when C7 is used alone or in combination, we determined various cutoff conditions through follow-up studies using various clusters and groups. This is expected to further enhance the usefulness of plasma C7. In addition, it was confirmed that the OS and PFS of NSCLC patients increased as the concentration of plasma C7 decreased. This pattern was similar to the pattern in which the OS and PFS increased as the PD-L1 TPS % increased. In other words, this suggests that the C7 protein might act as an important mediator that affects the survival of cancer patients, in a manner similar to that observed for the PD-1/PD-L1 ICI.

The role of plasma C7 in the tumor immune microenvironment

Complement activation can be initiated by classical, alternative, and lectin pathways, and eventually lead to the formation of the terminal complement complex or the membrane attack complex (MAC) [31]. The cleavage of complement C5 sequentially activates the terminal complement components C6, C7, C8, and C9 [31]. The binding and formation of the complex of C5b and C6 (C5b6) with C7 can initiate its

incorporation into the target membrane [31]; thus, C7 functions as a crucial limiting factor that controls the terminal cascade [32]. Here, we found that a significantly reduced plasma C7 level was observed in patients or animals exhibiting a good response to PD-1 ICI treatment and enhanced deposition of C7 in tumor tissues (Fig. 4E and F). Complement components are generally synthesized from the liver [33], but a large portion of circulating C7 originates from extrahepatic cells, including monocytes/macrophages, platelets, and fibroblasts, rather than from hepatic cells [32–34]. Therefore, it is reasonable to expect that a significant amount of circulating C7 in the blood would be consumed in anti-PD-1-treated patients or mice because of the enhanced complement cascade in tumor tissues. However, the synthesis of C7 from non-hepatic cells appeared to be compromised due to the blockade of immune cells by PD-1 or was not enough to compensate for the rate of C7 consumption. C7 is the rate-limiting factor that affects the effector function of the complement cascade. C7 biosynthesis is controlled by extrahepatic cells rather than hepatic cells, and is dependent on inflammation. This could explain why C7, rather than C6 and C9, could enable us to discriminate between cancer patients exhibiting a good oncologic response to the PD-1 blockade in a more effective manner.

Conclusions and expert recommendations

In summary, the deposition of plasma C7 on or around lung cancer cells affects the tumor immune environment, and this phenomenon is thought to affect the therapeutic response of PD-L1 ICIs in lung cancer cells. Thus, the quantitative measurement of plasma C7 concentrations in the blood plasma of lung cancer patients via ELISA enabled the prediction of the response to PD-1/PD-L1 ICIs and to overcome the disadvantages associated with the use of approved CDx, such as the ambiguity in the determined outcome. It has also been suggested for use as an alternative or adjuvant to CDx, especially to determine whether to treat NSCLC patients with pembrolizumab.

Companion diagnostics (CDx) takes a significant role in modern precision medication. It has clinical advantages in giving out adequate patients and adequate medicine at adequate timing.

PD-1/PD-L1 immune checkpoint inhibitor, an efficient treatment for NSCLC patients, has been developed along with CDx to analyze its PD-L1 expression level. Different PD-L1 expression levels among patients/groups made trouble setting proper stratification caused low prediction accuracy. Need for a new biomarker to resolve this disclosed disadvantage has arisen, and plasma C7 collected

from personalized patient profiling can play a major role as predictive diagnostics for PD-1/PD-L1 ICI.

Cancer often metastasizes to other several organs if proper treatment was not followed at proper timing. Many NSCLC patients who have not been treated with proper medication because of inaccurate current CDx show a low long-term survival ratio upon the second occurrence of metastatic diseases. The use of plasma C7 would guide NSCLC patients to proper treatment which would allow efficiently targeted prevention on secondary metastatic disease.

Immediate monitoring of change in cancer patients' tumor immune microenvironment which plays a pivotal role in oncogenesis, invasiveness, and even metastatic can be a successful approach to realize 3P medicine. Plasma C7 protein in the innate immune system can be analyzed through a noninvasive sampling method which has advantages over ordinary tissue biopsy that causes patient repulsion. Treatment algorithms tailored to the person that uses plasma C7 to frequent monitoring of the tumor immune microenvironment of cancer patients would be instrumental in deciding adequate timing for medication to prevent metastasis or worsening of cancer. In addition, plasma C7 can be analyzed at a comparatively low cost, and its results are clear to interpret. It would mutually benefit both hospital and patients that hospital could provide superior medical service at reasonable expense while patients and their families could prevent unnecessary treatment causing financial burden. These benefits will contribute to building robust personalization of medical services.

Conclusively, plasma C7 enables cancer control by tumor immune microenvironment monitoring and forms new stratification for PD-1/PD-L1 treatment algorithm which comes as a result of its noble screening method. It provides efficient medical service and an optimized medical economy followed which finally promotes the prosperity of 3P medicine.

Abbreviations 3P medicine: Predictive, preventive, and personalized medicine; C7: Complement component 7; PD-1: Programmed cell death protein 1; PD-L1: Programmed cell death ligand 1; ICI: Immune checkpoint inhibitor; CDx: Companion diagnostics; NSCLC: Non-small cell lung cancer; NCC: National Cancer Center; SMC: Samsung Medical Center; PFS: Progression-free survival; OS: Overall survival; TMB: Tumor mutation burden; MS: Mass spectroscopy; AGC: Automatic gain control; HCD: Higher-energy collisional dissociation; IACUC: Institutional Animal Care and Use Committee; NCCI: National Cancer Center Institute; TDLN: Tumor-draining lymph node; ECL: Enhanced chemiluminescence; AUC: Area under the curve; ACC: Accuracy; ROC: Receiver operating characteristics; N: Number; CR: Complete responder; PR: Partial responder; SD: Stable disease; PD: Progressive disease; responder: Responder with clinical benefit (PFS \geq 6 months); Non-responder: Non-responder without clinical benefit (PFS < 6 months); ADC: Adenocarcinoma; SqCC: Squamous cell carcinoma; Other: Other types of lung cancer; CRO: Contract research organization; CRA: Clinical research associate; SEN: Sensitivity; SPE: Specificity; PPV: Positive predictive value; NPV: Negative predictive value

Supplementary Information The online version contains supplementary material available at <https://doi.org/10.1007/s13167-021-00266-x>.

Author contribution This study was designed by JG Park, BK Choi, YJ Lee, SH Lee, and BC Yoo. Study material provision and patient recruitment were performed by YJ Lee and SH Lee. The data were collected and assembled by JG Park, BK Choi, YJ Lee, EJ Jang, SH Lee, and BC Yoo. All authors contributed to data analysis and interpretation. This manuscript was written by JG Park, BK Choi, YJ Lee, SH Lee, and BC Yoo. All authors contributed to the review and approved the final version of the manuscript. All authors had full access to all data and approved the submission of this manuscript for publication.

Funding This study was funded by research grants from the National Cancer Center, Republic of Korea (NCC-2010161, and NCC-2110480-1), and InnoBation Bio Co., Ltd. (202000380001).

Availability of data and material All raw data and materials are available from the corresponding authors upon reasonable request.

Code availability Not applicable

Declarations

Ethics approval This study was approved by the National Cancer Center Institutional Review Board (NCC-2017-0257) and the Samsung Medical Center Institutional Review Board (SMC-2018-04-048). All animal experiments were performed in accordance with the animal experimental guidelines and were approved by the Ethics Committee of the National Cancer Center, Republic of Korea.

Consent to participate Written informed consent was obtained for each volunteer to participate in the study.

Consent for publication Written informed consent was obtained from each volunteer for publishing the data.

Conflict of interest The authors declare no competing interests.


References

1. Cha E, Wallin J, Kowanz M. PD-L1 inhibition with MPDL3280A for solid tumors. In: *Semin Oncol*. WB Saunders; 2015:484–87. <https://doi.org/10.1053/j.seminoncol.2015.02.002>.
2. Gettinger SN, Shepherd FA, Antonia SJ, Brahmer JR, Chow LQM, Juergens RA, et al. First-line nivolumab (anti-PD-1; BMS-936558, ONO-4538) monotherapy in advanced NSCLC: Safety, efficacy, and correlation of outcomes with PD-L1 status. *J Clin Oncol*. 2014;32:8024. https://doi.org/10.1200/jco.2014.32.15_suppl.8024.
3. Genentech. FDA approves Genentech's Tecentriq as a first-line monotherapy for certain people with metastatic non-small cell lung cancer. May 18, 2020. Available from: <https://bit.ly/2ZfNjHK>
4. US FDA. FDA approves durvalumab for extensive-stage small cell lung cancer. March 30, 2020. Available from: <https://www.fda.gov/drugs/resources-information-approved-drugs/fda-approves-durvalumab-extensive-stage-small-cell-lung-cancer>
5. US FDA. FDA expands pembrolizumab indication for first-line treatment of NSCLC (TPS \geq 1%). April 11, 2019. Available from: <https://www.fda.gov/drugs/fda-expands-pembrolizumab-indication-first-line-treatment-nsclc-tps-1>
6. US FDA. FDA approves atezolizumab for first-line treatment of metastatic NSCLC with high PD-L1 expression. May 18, 2020. Available from: <https://www.fda.gov/drugs/resources-information-approved-drugs/fda-approves-atezolizumab-first-line-treatment-metastatic-nsclc-high-pd-l1-expression>
7. Horn L, Spigel DR, Vokes EE, Holgado E, Ready N, Steins M, et al. Nivolumab versus docetaxel in previously treated patients with advanced non-small-cell lung cancer: two-year outcomes from two randomized, open-label, phase III trials (CheckMate 017 and CheckMate 057). *J Clin Oncol*. 2017;35:3924. <https://doi.org/10.1200/JCO.2017.74.3062>.
8. Herbst RS, Baas P, Kim DW, Felip E, Perez-Gracia JL, Han JY, et al. Pembrolizumab versus docetaxel for previously treated, PD-L1-positive, advanced non-small-cell lung cancer (KEYNOTE-010): a randomised controlled trial. *Lancet*. 2016;387:1540–50. [https://doi.org/10.1016/S0140-6736\(15\)01281-7](https://doi.org/10.1016/S0140-6736(15)01281-7).
9. Spira AI, Park K, Mazières J, Vansteenkiste JF, Rittmeyer A, Ballinger M, et al. Efficacy, safety and predictive biomarker results from a randomized phase II study comparing MPDL3280A vs docetaxel in 2L/3L NSCLC (POPLAR). *J Clin Oncol*. 2015;33(15_suppl):8010. https://doi.org/10.1200/jco.2015.33.15_suppl.8010.
10. Rittmeyer A, Barlesi F, Waterkamp D, Park K, Ciardiello F, Von Pawel J, et al. Atezolizumab versus docetaxel in patients with previously treated non-small-cell lung cancer (OAK): a phase 3, open-label, multicentre randomised controlled trial. *Lancet*. 2017;389:255–65. [https://doi.org/10.1016/S0140-6736\(16\)32517-X](https://doi.org/10.1016/S0140-6736(16)32517-X).
11. Rangachari D, VanderLaan PA, Shea M, Le X, Huberman MS, Kobayashi SS, et al. Correlation between classic driver oncogene mutations in EGFR, ALK, or ROS1 and 22C3-PD-L1 \geq 50% expression in lung adenocarcinoma. *J Thorac Oncol*. 2017;12:878–83. <https://doi.org/10.1016/j.jtho.2016.12.026>.
12. Smith J, Robida MD, Acosta K, Vennapusa B, Mistry A, Martin G, et al. Quantitative and qualitative characterization of two PD-L1 clones: SP263 and E1L3N. *Diagnostic Pathol*. 2016;11:1–9. <https://doi.org/10.1186/s13000-016-0494-2>.
13. Jazieh AR, Bounedjar A, Bamefleh H, Alfayea T, Almaghraby HQ, Belarabi A, et al. Expression of immune response markers in Arab patients with lung cancer. *JCO Global Oncol*. 2020;6:1218–24. <https://doi.org/10.1200/GO.20.00107>.
14. Ilie M, Long-Mira E, Bence C, Butori C, Lassalle S, Bouhel L, et al. Comparative study of the PD-L1 status between surgically resected specimens and matched biopsies of NSCLC patients reveal major discordances: a potential issue for anti-PD-L1 therapeutic strategies. *Ann Oncol*. 2016;27:147–53. <https://doi.org/10.1093/annonc/mdv489>.
15. Munari E, Zamboni G, Marconi M, Sommaggio M, Brunelli M, Martignoni G, et al. PD-L1 expression heterogeneity in non-small cell lung cancer: evaluation of small biopsies reliability. *Oncotarget*. 2017;8:90123. <https://doi.org/10.18632/oncotarget.21485>.
16. Paz-Ares L, Langer CJ, Novello S, et al. Pembrolizumab (pembro) plus platinum-based chemotherapy (chemo) for metastatic NSCLC: tissue TMB (tTMB) and outcomes in KEYNOTE-021, 189, and 407. *Ann Oncol*. 2019;30:851–934. <https://doi.org/10.1093/annonc/mdz394.078>.
17. Torlakovic E, Lim HJ, Adam J, Barnes P, Bigras G, Chan AWH, et al. Interchangeability of PD-L1 immunohistochemistry assays: a meta-analysis of diagnostic accuracy. *Mod Pathol*. 2020;33:4–17. <https://doi.org/10.1038/s41379-019-0327-4>.
18. Tsimafeyeu I, Imyanitov E, Zavalishina L, Raskin G, Povilaitite P, Savelov N, et al. Agreement between PDL1 immunohistochemistry assays and polymerase chain reaction in non-small cell

- lung cancer: CLOVER comparison study. *Sci Rep.* 2020;10:1–8. <https://doi.org/10.1038/s41598-020-60950-2>.
19. Munari E, Zamboni G, Sighele G, Marconi M, Sommaggio M, Lunardi G, et al. Expression of programmed cell death ligand 1 in non-small cell lung cancer: comparison between cytologic smears, core biopsies, and whole sections using the SP263 assay. *Cancer Cytopathol.* 2019;127:52–61. <https://doi.org/10.1002/cncy.22083>.
 20. Li J, Jie HB, Lei Y, Gildener-Leapman N, Trivedi S, Green T, et al. PD-1/SHP-2 Inhibits Tc1/Th1 phenotypic responses and the activation of T cells in the tumor microenvironment. *Cancer Res.* 2015;75:508–18. <https://doi.org/10.1158/0008-5472>.
 21. Li B, Li F, Huangyang P, Burrows M, Guo K, Riscal R, et al. FBP1 loss disrupts liver metabolism and promotes tumorigenesis through a hepatic stellate cell senescence secretome. *Nat Cell Biol.* 2020;22:728–39. <https://doi.org/10.1038/s41556-020-0511-2>.
 22. Sawyers CL, Zhang Z, Karthaus WR, Lee YS, Gao VR, Wu C, et al. Tumor microenvironment-derived NRG1 promotes antiandrogen resistance in prostate cancer. *Cancer Cell.* 2020;38:279–96. <https://doi.org/10.1016/j.ccell.2020.06.005>.
 23. Gerner C, Brunmair J, Bileck A, Stimpfl T, Rabile F, Favero GD, et al. Metabo-tip: a metabolomics platform for lifestyle monitoring supporting the development of novel strategies in predictive, preventive and personalised medicine. *EPMA J.* 2021;1–13(12):1–20. <https://doi.org/10.1007/s13167-021-00241-6>.
 24. Kucera R, Pecan L, Topolcan O, Dahal AR, Costigliola V, Giordano FA, et al. Prostate cancer management: long-term beliefs, epidemic developments in the early twenty-first century and 3PM dimensional solutions. *EPMA J.* 2020;11:399–418. <https://doi.org/10.1007/s13167-020-00214-1>.
 25. Golubnitschaja O, Baban B, Boniolo G, Wang W, Bubnov R, Kapalla M, et al. Medicine in the early twenty-first century: paradigm and anticipation. *EPMA J.* 2016;7(1):23. <https://doi.org/10.1186/s13167-016-0072-4>.
 26. Aydin B, Caliskan A, Arga KY. Overview of Omics biomarkers in pituitary neuroendocrine tumors to design future diagnosis and treatment strategies. *EPMA J.* 2021;12:383–401. <https://doi.org/10.1007/s13167-021-00246-1>.
 27. Demark-Wahnefried W, Rogers LQ, Gibson JT, Harada S, Frugé AD, Oster RA, et al. Randomized trial of weight loss in primary breast cancer: impact on body composition, circulating biomarkers and tumor characteristics. *Int J Cancer.* 2020;146:2784–96. <https://doi.org/10.1002/ijc.32637>.
 28. Huizar CC, Raphael I, Forsthuber TG. Genomic, proteomic, and systems biology approaches in biomarker discovery for multiple sclerosis. *Cell Immunol.* 2020;358:104219. <https://doi.org/10.1016/j.cellimm.2020.104219>.
 29. Eisenhauer EA, Therasse P, Bogaerts J, Schwartz LH, Sargent D, Ford R, et al. New response evaluation criteria in solid tumours: revised RECIST guideline (version 1.1). *Eur J Cancer.* 2009;45:228–47. <https://doi.org/10.1016/j.ejca.2008.10.026>.
 30. Smits N. A note on Youden's J and its cost ratio. *BMC Med Res Methodol.* 2010;10:1–4. <https://doi.org/10.1186/1471-2288-10-89>.
 31. Würzner R. Modulation of complement membrane attack by local C7 synthesis. *Clin Exp Immunol.* 2000;121:8. <https://doi.org/10.1046/j.1365-2249.2000.01263.x>.
 32. Naughton MA, Walport MJ, Würzner R, Carter J, Alexander GJ, Goldman JM, et al. Organ-specific contribution to circulating C7 levels by the bone marrow and liver in humans. *Eur J Immunol.* 1996;26:2108–12. <https://doi.org/10.1002/eji.1830260922>.
 33. Colten HR, Strunk RC. Synthesis of complement components in liver and at extrahepatic sites. Complement in health and disease. Dordrecht: Springer; 1993. p. 127–58. https://doi.org/10.1007/978-94-011-2214-6_4.
 34. Morgan BP, Gasque P. Extrahepatic complement biosynthesis: where, when, and why? *Clin Exp Immunol.* 1997;107:1. <https://doi.org/10.1046/j.1365-2249.1997.d01-890.x>.

Publisher's note Springer Nature remains neutral with regard to jurisdictional claims in published maps and institutional affiliations.

Authors and Affiliations

Jae Gwang Park^{1,2} · Beom Kyu Choi³ · Youngjoo Lee⁴ · Eun Jung Jang^{1,5} · Sang Myung Woo^{3,5,6} · Jun Hwa Lee¹ · Kyung-Hee Kim^{5,7} · Heeyoun Hwang⁸ · Wonyoung Choi⁹ · Se-Hoon Lee¹⁰ · Byong Chul Yoo^{1,5} 

¹ Cancer Diagnostics Branch, Division of Clinical Research, Research Institute, National Cancer Center, 323 Ilsan-ro, Ilsandong-gu, Gyeonggi-do, Goyang-si 10408, Republic of Korea

² R&D Center, InnoBation Bio Co., Ltd., 14F, K-BIZ DMC Tower, 189, Seongam-ro, Mapo-gu, Seoul 03929, Republic of Korea

³ Biomedicine Production Branch, National Cancer Center, Goyang, Republic of Korea

⁴ Center for Lung Cancer, National Cancer Center, Goyang, Republic of Korea

⁵ Department of Cancer Biomedical Science, National Cancer Center Graduate School of Cancer Science and Policy, National Cancer Center, Goyang, Republic of Korea

⁶ Center for Liver and Pancreatobiliary Cancer, National Cancer Center, Goyang, Republic of Korea

⁷ Proteomics Core Facility, Research Core Center, Research Institute, National Cancer Center, Goyang, Republic of Korea

⁸ Research Center for Bioconvergence Analysis, Korea Basic Science Institute, 169-148, Gwahak-ro, Yuseong-gu, Daejeon 34133, Republic of Korea

⁹ Center for Clinical Trials, National Cancer Center, Goyang, Republic of Korea

¹⁰ Division of Hematology-Oncology, Department of Medicine, Samsung Medical Center, Sungkyunkwan University School of Medicine, 81, Irwon-ro, Gangnam-gu, Seoul, Republic of Korea